

LMI Based Wide Area TCSC Controller in Mitigating Small Signal Oscillations

D. Mondal, A. Chakrabarti, A. Sengupta

Abstract— This paper proposes a Linear Matrix Inequality (LMI) based H_∞ robust controller design employing Wide Area Measurement (WAM) based stabilizing signals as generator speed. A Three-input, Single-output (TISO) controller is designed for a Thyristor Controlled Series compensator (TCSC) in order to mitigate small signal oscillations in a multimachine power system. The controller design has been carried out based on the H_∞ mixed-sensitivity formulation in a LMI framework with pole-placement constraint. The small signal performance of the test system has been examined employing eigenvalue analysis as well as time domain response. The designed controller is found to be robust against disturbances like varying generations as well as load power demand.

Index Terms— H_∞ Robust Controller, Linear Matrix Inequality, Small Signal Oscillations, Thyristor Controlled Series Compensator, Wide Area Measurement

I. INTRODUCTION

The problem of low frequency (0.2-1.0 Hz) electromechanical oscillations is inherent in electric power systems. These oscillations may sustain and may grow to cause severe system outage if adequate damping is not available [1]. Traditionally, potential benefits of using Power System Stabilizer (PSS) to damp these oscillations for enhancing power system stability are well known [2]. With the development of power electronics, Flexible Alternating Current Transmission System (FACTS) devices [3] have gathered much attention from the researchers in this issue. Thyristor Controlled Series Compensator (TCSC), a series controlled FACTS device, is increasingly applied [4] for this purpose in long transmission lines of modern power systems.

It is well known that the conventional damping controller design synthesis is simple but tends to lack of robustness even after careful tuning. Attempts have been made in [5] to design a new PSS for damping power system oscillations focusing on inter-area modes using global signals. In [6] it has been reported that an optimum and weighted combination of local

and global signals could successfully be used for controller design of PSS and TCSC. A mixed-sensitivity based LMI approach using H_∞ techniques has been applied in [7] to design inter-area damping controller employing a Superconducting Magnetic Energy Storage (SMES) device. A Multiple-input, Single-output (MISO) robust controller design has been proposed in [8] for a TCSC to improve the damping of the inter-area modes. The recent advances in Wide Area Measurement (WAM) technologies using Synchronized Phasor Measurement (SPM) units with PSS and FACTS devices have been implemented for various problems in modern power systems [9]-[10].

Thus, there is a strong need to develop new controllers which are robust and can use system-wide multiple input signals from remote nodes and have satisfactory contribution on small signal oscillations. This paper addresses this problem and a Three-input, Single-output (TISO) WAM based H_∞ controller for a TCSC has been designed in LMI framework in order to robust damping of small signal oscillations of a multimachine power system. The transmission delay [11] associated with the wide area measurement signals are also incorporated in the design.

The paper is organized as follows; section II describes the general small signal modeling of multimachine system with TCSC device. The theory of mixed-sensitivity based robust controller design in LMI framework is explained in section III. The identification of critical swing mode prior to application of controller and the design procedure of robust damping controller for a TCSC have been illustrated in section IV and subsequently robust performance of the controller is examined in this section. In section V, theory of the Wide Area Measurement (WAM) has been introduced briefly.

II. SYSTEM MODELING

A. Multimachine small signal model with TCSC

The small signal modeling of a multimachine system with IEEE-Type I exciter has been described in [12]. The linearized dynamic model of the system for eigenvalue analysis are represented by the following state-space equations

$$\Delta \dot{X} = A_1 \Delta X + B_1 \Delta I_g + B_2 \Delta V_g + E_1 \Delta U \quad (1)$$

$$0 = C_1 \Delta X + D_1 \Delta I_g + D_2 \Delta V_g \quad (2)$$

$$0 = C_2 \Delta X + D_3 \Delta I_g + D_4 \Delta V_g + D_5 \Delta V_l \quad (3)$$

$$0 = D_6 \Delta V_g + D_7 \Delta V_l \quad (4)$$

D. Mondal is with the Department of Electronics and Instrumentation Engineering, Haldia Institute of Technology, Purba Medinipur, Haldia-721657, India (e-mail: mondald12@yahoo.in).

A. Chakrabarti is with the Department of Electrical Engineering, Bengal Engineering and Science University, Howrah-711103, India (e-mail: achakrabarti58@gmail.com).

A. Sengupta is with the Department of Electrical Engineering, Bengal Engineering and Science University, Howrah-711103, India (e-mail: sgaparajita@gmail.com).

Here equations (1) and (2) represent the linearized differential equations and linearized stator algebraic equations of the machine, while equations (3) and (4) correspond to the linearized network equations pertaining to the generator buses and the load buses. The variable ΔX contains machine states and the state corresponding to PSS.

The basic TCSC configuration consists of a fixed series capacitor bank C in parallel with a Thyristor Controlled Reactor (TCR) as shown in Fig. 1. The series reactance of the TCSC [13] is adjusted through appropriate variation of the conduction angle (σ) to keep the specified amount of active power flow across the series compensated line. With the installations of a TCSC device, the TCSC power flow equations are to be additionally included with the network equation (4). The TCSC linearized power flow equations at the node s can be obtained by the following expression

$$0 = \begin{bmatrix} \frac{\partial P_s}{\partial \theta_s} & \frac{\partial P_s}{\partial V_s} & \frac{\partial P_s}{\partial \alpha} \\ \frac{\partial Q_s}{\partial \theta_s} & \frac{\partial Q_s}{\partial V_s} & \frac{\partial Q_s}{\partial \alpha} \\ \frac{\partial P_{st}}{\partial \theta_s} & \frac{\partial P_{st}}{\partial V_s} & \frac{\partial P_{st}}{\partial \alpha} \\ \frac{\partial Q_{st}}{\partial \theta_s} & \frac{\partial Q_{st}}{\partial V_s} & \frac{\partial Q_{st}}{\partial \alpha} \end{bmatrix} \begin{bmatrix} \Delta \theta_s \\ \Delta V_s \\ \Delta \alpha \end{bmatrix} \quad (5)$$

$$\text{where } P_{st} = V_s^2 g_{st} - V_s V_t (g_{st} \cos \theta_{st} + b_{st} \sin \theta_{st}) \quad (6)$$

$$\text{and } Q_{st} = -V_s^2 b_{st} - V_s V_t (g_{st} \sin \theta_{st} - b_{st} \cos \theta_{st}) \quad (7)$$

Similarly, the linearized power flow equations for the node t can be obtained by replacing t for s .

$$\text{Here, } Y_{st}^* = \frac{1}{R_{st} + j(X_{st} - X_{TCSC})} = \frac{R_{st} + j(X_{st} + X_{TCSC})}{R_{st}^2 + (X_{st} + X_{TCSC})^2} \\ = g_{st} - jb_{st} \quad (8)$$

where X_{TCSC} is the TCSC equivalent reactance.

$$\text{Again } \frac{\partial P_s}{\partial \alpha} = -\frac{\partial P_{st}}{\partial \alpha} \\ = -V_s^2 \frac{\partial g_{st}}{\partial \alpha} + V_s V_t (\cos \theta_{st} \frac{\partial g_{st}}{\partial \alpha} + \sin \theta_{st} \frac{\partial b_{st}}{\partial \alpha}) \quad (9)$$

Also $\frac{\partial P_{st}}{\partial \theta_s} = -\frac{\partial P_s}{\partial \theta_s}$ and $\frac{\partial P_{st}}{\partial V_s} = -\frac{\partial P_s}{\partial V_s}$ is true for the line between node s and t where TCSC is installed. The expression for $\frac{\partial g_{st}}{\partial \alpha}$ and $\frac{\partial b_{st}}{\partial \alpha}$ can be obtained from (8).

Eliminating ΔI_g from (1)-(4), the overall system matrix for an m -machine system can be obtained as

$$[A_{TCSC}]_{(9m+1) \times (9m+1)} = [A'] - [B'] [D']^{-1} [C'] \quad (10)$$

$$\text{where } A' = A_1 - B_1 D_1^{-1} C_1, B' = [B_2 - B_1 D_1^{-1} D_2 \ 0],$$

$$C' = \begin{bmatrix} K_2 \\ 0 \end{bmatrix} \text{ and } D' = \begin{bmatrix} K_1 & D_5 \\ D_6 & D_7 \end{bmatrix} \text{ with}$$

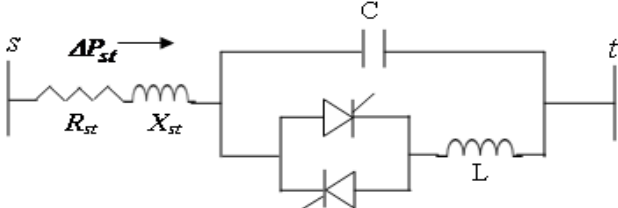


Fig. 1 TCSC module between node s and t

$$K_1 = [D_4 - D_3 D_1^{-1} D_2] \text{ and } K_2 = [C_2 - D_3 D_1^{-1} C_1].$$

Therefore, linearized state-space model of the multimachine system including TCSC power flow equations can be obtained as

$$\Delta \dot{X} = A_{TCSC} \Delta X + E_1 \Delta U \quad (11)$$

$$\Delta Y = C \Delta X \quad (12)$$

III. PROBLEM FORMULATION

A. Mixed-Sensitivity Based Robust Controller Design: an LMI Approach

The closed-loop system together with the H_∞ controller based on the standard mixed-sensitivity problem is proposed in Fig. 2. The problem is to minimize a weighted mixed-sensitivity transfer function $S(s) = [I - G(s)K(s)]^{-1}$, which ensures disturbance rejection and $K(s)S(s) = K(s)[I - G(s)K(s)]^{-1}$ that handles the robustness issues and minimizes the control effort. This mixed-sensitivity design approach associated with H_∞ control theory gives an internally stabilizing controller $K(s)$ which meets the following requirement [14]

$$\left\| \begin{bmatrix} W_1(s)S(s) \\ W_2(s)K(s)S(s) \end{bmatrix} \right\|_\infty < \gamma \quad (13)$$

where γ is the bound on H_∞ norm. $W_1(s)$ and $W_2(s)$ are weights for shaping the characteristics of the closed-loop plant.

The state space description of the augmented plant is represented by

$$\dot{x}_p = A_p x_p + B_{p1} d + B_{p2} u \quad (14)$$

$$z = C_{p1} x_p + D_{p11} d + D_{p12} u \quad (15)$$

$$y = C_{p2} x_p + D_{p21} d + D_{p22} u \quad (16)$$

where x_p is the state vector of the plant $G(s)$, u is the plant input, y is the measured signal modulated by the disturbance input d and z is the controlled output.

The controller $K(s)$ can be realized by the following state space form

$$\dot{\hat{x}} = A_k \hat{x} + B_k y \quad (17)$$

$$u = C_k \hat{x} + D_k y \quad (18)$$

The state space representation of the closed-loop plant is then given by

$$\dot{\chi} = A_{cl} \chi + B_{cl} d \quad (19)$$

$$z = C_{cl} \chi + D_{cl} d \quad (20)$$

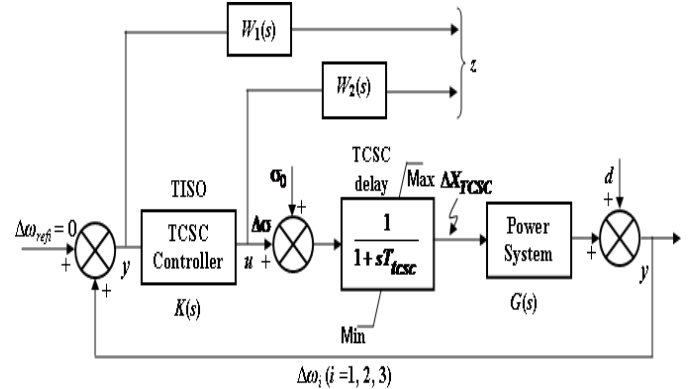


Fig. 2 The closed-loop system along with mixed-sensitivity output disturbance attenuation based H_∞ controller

where $\dot{X} = \begin{bmatrix} \dot{x}_p \\ \dot{x} \end{bmatrix}$, $A_{cl} = \begin{bmatrix} A_p + B_{p2}D_kC_{p2} & B_{p2}C_k \\ B_kC_{p2} & A_k \end{bmatrix}$;

$B_{cl} = \begin{bmatrix} B_{p1} + B_{p2}D_kD_{p21} \\ B_kD_{p21} \end{bmatrix}$; $C_{cl} = [C_{p1} + D_{p12}D_kC_{p2} \quad D_{p12}C_k]$;

$D_{cl} = D_{p11} + D_{p12}D_kD_{p21}$. Without loss of generality, D_{22} can be set to zero to make the derivation simpler [15] and the plant becomes strictly proper. The transfer function between 'd' to 'z' can be described as

$$T_{zd} = \begin{bmatrix} W_1(s)S(s) \\ W_2(s)K(s)S(s) \end{bmatrix} = C_{cl}(sI - A_{cl})^{-1}B_{cl} + D_{cl} \quad (21)$$

The objective of the mixed-sensitivity problem is to find an internally stabilizing controller $K(s)$ that minimizes the transfer function between 'd' to 'z' and is given by

$$\|T_{zd}\|_{\infty} < \gamma \quad (22)$$

In an LMI formulation, the equivalent objective (22) can be achieved in the sub-optimal sense if there exist a solution $X_{cl} = X_{cl}^T > 0$ such that the *bounded real lemma* [16] given by

$$\begin{bmatrix} A_{cl}^T X_{cl} + X_{cl} A_{cl} & B_{cl} & X_{cl} C_{cl}^T \\ B_{cl}^T & -I & D_{cl}^T \\ C_{cl} X_{cl} & D_{cl} & -\gamma^2 I \end{bmatrix} < 0 \quad (23)$$

is satisfied and the resulting controller design problem reduces to an LMI problem.

In an LMI frame work a class of convex region of the complex plane called LMI region can be assigned by clustering all the closed-loop poles inside a conic sector (Fig. 3) which ensures that the damping ratio of poles lying in this sector is at least $\zeta = \cos \frac{\theta}{2}$. The problem therefore reduces to minimization of γ under LMI based H_{∞} control with pole placement constraints. Pole clustering in LMI regions can be formulated as an LMI optimization problem, a *convex semidefinite programming* that is easily tractable with interior-point optimization technique [17].

It is shown in [18] that the state matrix, A_{cl} of the closed loop plant, has all its poles inside the conical sector if and only if there exists $X_c = X_c^T > 0$ such that

$$\begin{bmatrix} \sin \frac{\theta}{2} (A_{cl} X_c + X_c A_{cl}^T) & \cos \frac{\theta}{2} (A_{cl} X_c - X_c A_{cl}^T) \\ \cos \frac{\theta}{2} (X_c A_{cl}^T - A_{cl} X_c) & \sin \frac{\theta}{2} (A_{cl} X_c + X_c A_{cl}^T) \end{bmatrix} < 0 \quad (24)$$

or equivalently this can be expressed in Kronecker product form as shown in (25)

$$[\eta \otimes A_{cl} X_c + \eta^T \otimes X_c A_{cl}^T] < 0 \quad (25)$$

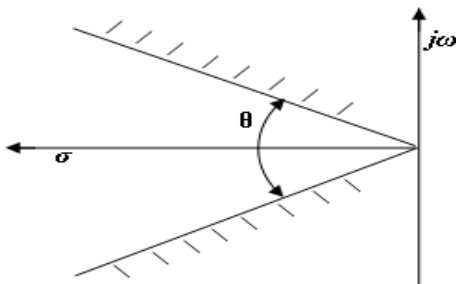


Fig. 3 Conic sector LMI region of closed loop poles

where $\eta = \begin{bmatrix} \sin \frac{\theta}{2} & \cos \frac{\theta}{2} \\ -\cos \frac{\theta}{2} & \sin \frac{\theta}{2} \end{bmatrix}$

The inequalities in (23) and (25) are not jointly convex as the solutions $X_{cl} \neq X_c$. The convexity can be accomplished by seeking a common solution, $X_{cl} = X_c = X_d$. It is to be noted that the inequalities in (23) and (25) contain non-linear terms $A_{cl} X_d$ and $C_{cl} X_d$ (A_{cl} and C_{cl} contain unknown matrices of the controller in (17)-(18)) and the resulting problem therefore cannot be handled by LMI optimization directly. To convert the problem into a linear one, a change of controller variables is necessary. The detailed analysis of this transformation has been shown in [18]-[19] which give the following simplified LMI's in terms of new controller variables:

$$\begin{bmatrix} Q & I \\ I & S \end{bmatrix} > 0 \quad (26)$$

$$\begin{bmatrix} \Pi_{11} & \Pi_{21}^T \\ \Pi_{21} & \Pi_{22} \end{bmatrix} < 0 \quad (27)$$

$$[\eta \otimes \Psi + \eta^T \otimes \Psi^T] < 0 \quad (28)$$

Here

$$\Pi_{11} = \begin{bmatrix} A_p Q + Q A_p^T + B_{p2} \hat{C} + \hat{C}^T B_{p2}^T & B_{p1} + B_{p2} \hat{D} D_{p21} \\ (B_{p1} + B_{p2} \hat{D} D_{p21})^T & -\gamma I \end{bmatrix}$$

$$\Pi_{21} = \begin{bmatrix} \hat{A} + (A_p + B_{p2} \hat{D} C_{p2})^T & S B_{p1} + \hat{B} D_{p21} \\ C_{p1} Q + D_{p12} \hat{C} & D_{p11} + D_{p12} \hat{D} D_{p21} \end{bmatrix}$$

$$\Pi_{22} = \begin{bmatrix} A_p^T S + S A_p + \hat{B} C_{p2} + C_{p2}^T \hat{B}^T & (C_{p1} + D_{p12} \hat{D} C_{p2})^T \\ C_{p1} + D_{p12} \hat{D} C_{p2} & -\gamma I \end{bmatrix}$$

with $\Psi = \begin{bmatrix} A_p Q + B_{p2} \hat{C} & A_p + B_{p2} \hat{D} C_{p2} \\ \hat{A} & S A_p + \hat{B} C_{p2} \end{bmatrix}$

The new controller variables are defined in [18] as

$$\hat{A} = N A_k M^T + N B_k C_{p2} Q + S B_{p2} C_k M^T + S (A_p + B_{p2} D_k C_{p2}) Q \quad (29)$$

$$\hat{B} = N B_k + S B_{p2} D_k \quad (30)$$

$$\hat{C} = C_k M^T + D_k C_2 Q \quad (31)$$

$$\hat{D} = D_k \quad (32)$$

where Q , S , M and N are submatrices of X_d . The LMIs in (26)-(28) are solved for \hat{A} , \hat{B} , \hat{C} and \hat{D} employing interior-point optimization methods. Once \hat{A} , \hat{B} , \hat{C} and \hat{D} are obtained the controller variables A_k , B_k , C_k and D_k are recovered from \hat{A} , \hat{B} , \hat{C} and \hat{D} by solving (29)-(32).

IV. RESULTS AND PERFORMANCE STUDY

A. Computation of Eigenvalues Prior to Application of H_{∞} TCSC controller

The power system under consideration (Fig. 4) is widely used in literature [12] for study of small signal oscillations. The proposed system has a total 21 numbers of eigenvalues for the base case and is listed in Table I. Here 2 numbers of eigenvalues (mode #1) are identified as electromechanical swing modes [20]. It is evident that the damping ratio of this

swing mode #1 is smallest compared to other modes and is referred to as the *critical swing mode*.

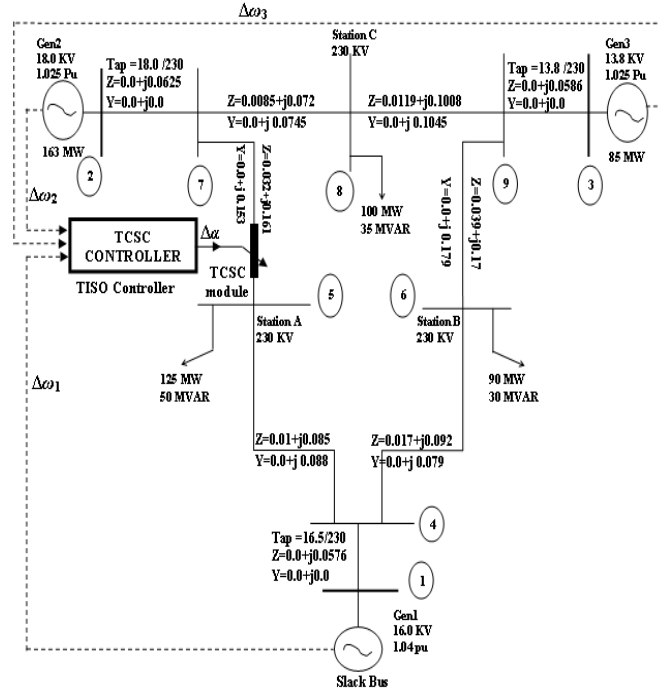


Fig. 4. WSCC 3 machine, 9 bus system with TCSC controller

Therefore, behavior of this mode is of prime concern for the study of the small signal oscillation problem of the system. The TCSC has been installed in a line between bus #5 and #7. The compensation of the TCSC was calculated to be 56%.

B. Design of Robust Damping Controller

The LMI formulation described in section III is now applied to the WSCC 3 machine, 9 bus study system. The original system has a total of 28 states including one state for the TCSC delay and three states for the transmission delay blocks. The corresponding LMI based controller would be of a higher order than this. The plant model is hence reduced to a 6-th order equivalent using square-root balanced truncation technique [15]. Applying standard mixed-sensitivity problem guidelines, the weights $W_1(s)$ and $W_2(s)$ are worked out to be:

$$W_1(s) = \frac{10}{0.15s + 15}; \quad W_2(s) = \frac{2s + 0.02}{0.15s + 15}$$

TABLE I
EIGEN VALUES AT NOMINAL CASE

#	Eigen value (λ)	Frequency (f) Hz	Damping ratio (ζ)
1	-2.4892 ± j10.8650	1.7290	0.2233
2	-5.1617 ± j11.2755	1.7943	0.4162
3	-5.3063 ± j10.3299	1.6438	0.4569
4	-5.6837 ± j10.3601	1.6486	0.4810
5	-5.5957 ± j10.3330	1.6443	0.4762
6	-2.5226	0	1.0000
7	0.0000	0	1.0000
8	-0.4087 ± j 0.8293	0.1320	0.4421
9	-0.4759 ± j 0.5616	0.0894	0.6465
10	-0.4164 ± j 0.6618	0.1053	0.5325
11	-3.2258	0	1.0000
12	-1.8692	0	1.0000
13	-1.6667	0	1.0000

The multiobjective H_∞ synthesis program for disturbance rejection and control effort optimization feature of LMI was accessed by suitably chosen arguments of the function *hinfnmix* of the *LMI Toolbox* in MATLAB [21]. The pole placement objective in LMI (24) has been achieved by defining the conical sector with $\frac{\theta}{2} = 67.5^\circ$, which provides a desired minimum damping $\zeta = 0.39$ for all the closed-loop poles.

The order of the controller obtained from the LMI solution was equal to the reduced plant order plus the order of the weights, which was quite high posing difficulty in practical implementation. Therefore, the controller was reduced to a fourth-order one by the balanced truncation without significantly affecting the frequency response. The state variable representation of the three-input, one-output controller for the TCSC is given in the Appendix A.1. This reduced-order controller has been tested on the full order system against varying generations and load power changes.

C. Robust Performance Evaluation of the WAM Controller

To examine robust performance of the WAM controller, an eigenvalue analysis of the system has been carried out under different operating scenarios. At first, the real and reactive power demand at bus #5 is increased to 20 % and next to 50 % from its nominal value. It has been observed that with this variation of load, damping ratio is reduced significantly but a satisfactory enhancement of damping has been achieved with installation of the WAM based TCSC controller. Secondly, the effect of generation drop on small signal oscillations of the system has been investigated by reducing the total real power generation of Gen #2 and #3 together to 20 % and further to 40%. It has been found that the damping ratio and hence the stability of the system has been deteriorated with generation drop and improved adequately in the presence of the controller. Table II contains the results for both without and with control conditions.

The performance robustness of the controller is further demonstrated by plotting the angular speed response of machine #2 for simulation time 7 sec (Fig. 5). It has been observed that the obtained LMI based WAM TCSC controller imparted acceptable settling time for both the cases of disturbances. Therefore, the performance of the designed TCSC controller appears to be robust and adequate against varying operating conditions.

TABLE II
DAMPING RATIO OF THE CRITICAL SWING MODE WITHOUT AND WITH WAM CONTROLLER

Power system disturbances		Damping ratio	
		Without control	With WAM TCSC controller
Load increase	20 % ($P_L = 1.50$, $Q_L = 0.6$)	0.21856	0.27482
	50 % ($P_L = 1.87$, $Q_L = 0.75$)	0.20899	0.2509
Generation drop	Total 20 %	0.21126	0.26594
	Total 40 %	0.19489	0.23227

VI. CONCLUSIONS

In this paper the design of a mixed-sensitivity based H_∞ controller in LMI framework is proposed for robust damping of a critical swing mode of a multimachine power system. The wide-area measurement based TSO robust damping controller is designed for a TCSC considering remote inputs as machine speed. The signal transmission delays for the remote measurement signals were incorporated by modelling it to an equivalent first-order filter. The robust performance of the controller has been verified through eigenvalue as well as the time domain analysis against small and wide variations of power system disturbances. The proposed technique can be implemented for the design of other WAM based FACTS controllers.

APPENDIX A

A.1 LMI based WAM TISO TCSC controller

The state-space representation of the three-input, one-output WAM controller for the TCSC

$$A_k = \begin{bmatrix} -1937.5 & -944.73 & -1482.2 & 322.09 \\ 819.12 & -2.4052 & -51.453 & 11.332 \\ 312.84 & -12.821 & -6113.6 & 1993.5 \\ -29.652 & 1.7648 & 1014.6 & -435.59 \end{bmatrix}$$

$$B_k = \begin{bmatrix} 754.61 & 228.95 & 77.087 \\ 26.349 & -7.600 & 4.210 \\ -4.452 & -225.63 & 197.92 \\ 3.579 & 22.91 & -61.44 \end{bmatrix}$$

$$C_k = [-792.34 \quad -27.744 \quad -300.17 \quad 65.674]$$

$$D_k = [0.002833 \quad 0.00000761 \quad 0.0050914]$$

A.2 Parameters of PSS and TCSC module

$K_{PSS} = 10$ (PSS gain); $T_1|_{PSS} = 0.4$ sec. (lead time);

$T_2|_{PSS} = 0.15$ sec. (lag time); $XL = 0.00491$ pu;

$XC = 0.02835$ pu; $T_{TCSC} = 17$ ms. (TCSC internal delay).

REFERENCES

- [1] P. Kundur, *Power System Stability and Control*. New York: McGraw-Hill; 1994.
- [2] P. Kundur, M. Klein, G. j. Rogers and M. S. Zywno, "Application of power system stabilizers for enhancement of overall system stability," *IEEE Trans. on Power Systems*, vol. 4, no. 2, 1989, pp. 614-626.
- [3] N. G. Hingorani and L. Gyugyi. *Understanding FACTS: Concepts and technology of Flexible AC Transmission System*. IEEE Press; 2000.
- [4] M. O. Hassan, Z. A. Zakaria and S. J. Cheng, "Impact of TCSC on enhancing power system stability," *IEEE Power and Energy Conference, APPEEC 2009*; pp. 1-6.
- [5] M. E. Aboul-Ela, A. A. Sail am, J. D. McCalley and A. A. Fouad, "Damping controller design for power system oscillations using global signals," *IEEE Trans. on Power System*, vol. 11, no.2, May 1996, pp. 767-773.
- [6] J. Chow, J. Sanchez-Gasca, H. Ren, and S. Wang, "Power system damping controller design using multiple input signals," *IEEE Contr. Syst. Mag.*, vol. 20, Aug. 2000, pp. 82-90.
- [7] B. C. Pal, A. A. Coonick, I. M. Jaimoukha, and H. El-Zobaidi, "A Linear Matrix Inequality Approach to Robust Damping Control Design in Power Systems with Superconducting Magnetic Energy Storage Device," *IEEE Transactions on power systems*, vol. 15, no. 1, Feb. 2000, pp. 356-362.

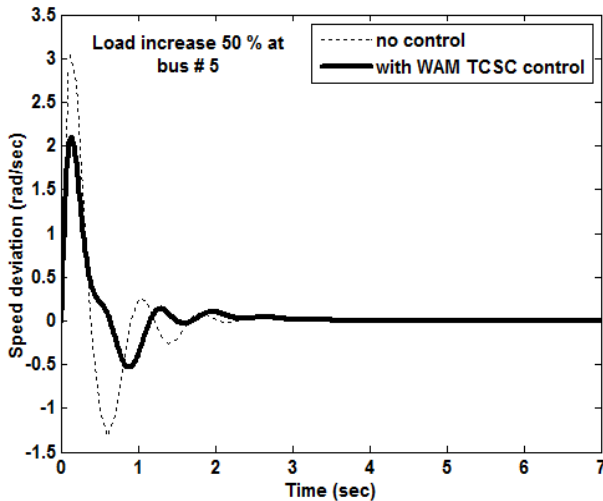


Fig. 5 (a) Dynamic response for load increase 50 % at bus #5

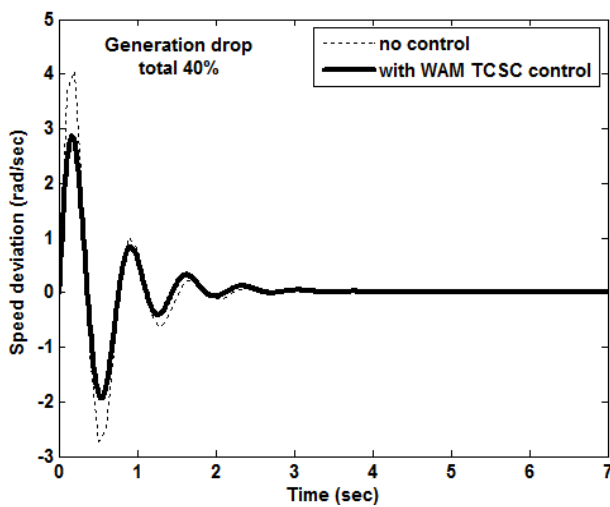


Fig. 5 (b) Dynamic response for gen. drop total 40 % of Gen #2 & Gen #3

V. THEORY OF WIDE AREA MEASUREMENT (WAM)

The wide area signals measured from remote power system substation can be transmitted to the centralized TCSC controller by fibre optic or Ethernet communication with secure and reliably. One of the major concerns of wide area communication is the transportation delay. The delays for the remote signals were modelled here by a first-order filter in the controller feedback and incorporated with the system states. In this work a uniform delay of value maximum 0.5s has been assumed for all remote signals.

It is to be noted that this communication delay is overcome nowadays by synchronizing wide area measured signals with Global Position Satellite System (GPS) technology. The measured synchronized speed signals ($\Delta\omega$) from remote substations may be transmitted over a dedicated communication line through the modems to the centralized controller. A 4800 or 9600 baud communication line can support the transmission at the rate of about every 2-5 cycles (40 - 100 msec) of the fundamental frequency (50 Hz). Considering that the usual power system dynamic phenomena fall in the range of 0.2 - 2.5 Hz, it is possible to observe and control in real-time the power system dynamic phenomena with high fidelity at the control centre.

- [8] B. Chaudhuri and B. C. Pal, "Robust damping of multiple swing modes employing global stabilizing signals with a TCSC," *IEEE Trans. on power systems*, vol. 19, no. 1, Feb. 2004, pp. 499-506.
- [9] I. Kamwa, R. Grondin and Y. Hebert, "Wide-area measurement based stabilizing control of large power systems—A decentralized/hierarchical approach," *IEEE Trans. Power Syst.*, vol. 16, Feb. 2001, pp. 136–153.
- [10] F. Okou, L. A Dessaint and O. Akhrif, "Power system stability enhancement using a wide-area signals based hierarchical controller," *IEEE Trans. on Power System*, vol. 20, Aug. 2005, pp. 1465-1477.
- [11] H. Wu, S. Tsakalis and G. T. Heydt, "Evaluation of time delay effects to wide-area power system stabilizer design," *IEEE Transactions on power systems*, vol. 10, no. 4, Nov. 2004, pp. 1935-1941.
- [12] P. W. Sauer and M. A. Pai, *Power system dynamics and stability*; Pearson Education Pte. Ltd.: Singapore, 1998.
- [13] C. R. Fuerte-Esquivel, E. Acha and H. Ambriz-Pe'rez, "A thyristor controlled series compensator model for the power flow solution of practical power networks," *IEEE Trans on power systems*, vol. 15, no. 1, 2000, pp. 58-64.
- [14] S. Skogestad and I. Postlethwaite, *Multivariable Feedback Control Analysis and Design*: John Wiley and Sons. 1996.
- [15] K. Zhou, J. Doyle and K. Glover, *Robust and Optimal Control*: Prentice Hall, 1995.
- [16] P. Gahinet and P. Apkarian, "A linear matrix inequality approach to H_∞ control," *Int. J. Robust Nonlinear Contr.*, vol. 4, no. 4, Apr. 1994, pp. 421–448.
- [17] Y. Nesterov and A. Nemirovski, *Interior Point Polynomial Methods in Convex Programming; Theory and Applications*. Philadelphia, PA: SIAM, 1994.
- [18] M. Chilali and P. Gahinet, " H_∞ design with pole placement constraints: An LMI approach," *IEEE Transaction on Automatic Control*, vol. 41, no. 3, Mar. 1996, pp. 358-367.
- [19] C. Scherer, P. Gahinet and M. Chilali, "Multiobjective output-feedback control via LMI optimization," *IEEE Trans. on Automatic Control*, vol. 42, no. 7, July 1997, pp. 896-911.
- [20] E. Z. Zhou, O. P. Malik and G. S. Hope, "A reduced-order iterative method for swing mode computation," *IEEE Trans. on Power Systems*, vol. 6, no. 3, 1991, pp. 1224-1230.
- [21] Matlab Users Guide, *The Math Works Inc.*, USA, 1998.

BIOGRAPHIES



Debasish Mondal (AM'098104 7) received his degree of engineering and Master of Engineering in 1998 and 2000, respectively. He has 12 years of industrial and teaching experience. He holds a permanent post of Assistant Professor at the Haldia Institute of Technology, India. His research interests on the areas like power systems stability, soft computing and robust control. He is an associate member of the Institution of Engineers (India).



Abhijit Chakrabarti (F'16040 3) received B.E., M.Tech. and Ph.D. (Tech) degrees in 1978, 1987 and 1991 respectively. He is a professor at the Department of Electrical engineering, Bengal Engineering and Science University, India. He has 30 years of research and teaching experience and has around 120 research papers in National and International journal and conferences. He has active interest on the areas like power systems, power electronics and circuit theory. He is a fellow of the Institution of Engineers (India).



Aparajita Sengupta (M'41432862) received her B.E., M.Tech. and Ph.D. degrees in 1992, 1994 and 1997, respectively. She is employed in teaching and research at the Department of Electrical Engineering, Bengal Engineering and Science University, India, for 14 years. Her areas of interest are power system, robust control and nonlinear control and state estimation methods. She is a member of the IEEE.